

Natural Zeolites Modified with Silver Nanoparticles as Promising Sorbents with Antibacterial Properties



L. K. Patrylak, A. V. Yakovenko, B. O. Nizhnik, O. P. Pertko, V. A. Povazhnyi, D. S. Kamenskyh, and O. V. Melnychuk

Abstract To improve the porous properties of natural Ukrainian clinoptilolite, it was treated with ethylenediamine tetraacetic acid. Ag-containing zeolite and gamma-alumina samples were obtained by their impregnation with silver nitrate and the thermal decomposition of the latter. Synthesized samples were investigated by using SEM, TEM, low temperature nitrogen adsorption/desorption, FTIR spectroscopy, and DTA/TG. Nanosized silver particles of 5–10 nm were detected on the zeolite sample only. Total viable count determination was used to investigate the antibacterial properties of the samples. Water samples from three Kyiv's lakes (Sonyachne, Svyatoshynske, and Radunka) were used in the study. In comparison with Ag–Al₂O₃, Ag-containing zeolite sample demonstrates better performance in antibacterial activity. The latter can be caused by the nanodimensionality of Ag species on the zeolite surface as well as by the stronger interaction of silver with zeolite cations.

1 Introduction

Today, more than eighty types of natural zeolites are known [1, 2]. The latter, in contrast to synthetic zeolites, usually contain a number of impurities from other rocks. Clinoptilolite, as a zeolite of the heulandite group, finds considerable application [1–4] in various fields. It is one of the most stable and common natural zeolites in the world. Big deposits of clinoptilolite are available in the Transcarpathian region of Ukraine. Despite its significant deposits, the use of the latter as a basis for catalysts and sorbents is currently insignificant. The shortcomings of the porous structure of

L. K. Patrylak (✉) · A. V. Yakovenko · B. O. Nizhnik · O. P. Pertko · V. A. Povazhnyi · D. S. Kamenskyh · O. V. Melnychuk
V.P. Kukhar Institute of Bioorganic Chemistry and Petrochemistry of National Academy of Sciences of Ukraine, Kyiv, Ukraine
e-mail: lkpg@ukr.net

L. K. Patrylak · B. O. Nizhnik · O. V. Melnychuk
National Technical University of Ukraine “Igor Sikorskyi Kyiv Polytechnic Institute”, Kyiv, Ukraine

the clinoptilolite, on the other hand, limit the widespread usage of Ukrainian natural zeolites.

In the past, silver in all of its forms has been utilized either alone or in conjunction with other technologies as an antibacterial agent [5, 6]. Utilizing this metal as silver nitrate or silver sulfadiazine has been studied for use in food packaging to prevent contamination, in home appliances such as refrigerators and washing machines, and in several industrial applications [6–10]. With the development of new knowledge in nanotechnology and related sciences [11], it becomes possible to explore the antibacterial potential of Ag nanoparticles deposited on carriers, too.

Silver nanoparticles have been imposed as an excellent antimicrobial agent being able to combat bacteria *in vitro* and *in vivo* causing infections [5].

Ag nanoparticles have especially been employed as antibacterials, antifungals, and antioxidants in agriculture and medicine. Ag demonstrates antibacterial activity against gram-positive and gram-negative bacteria. However, the exact mechanism of such behavior is still under discussion. The existing experimental evidence supports different mechanisms that consider the physicochemical properties of Ag nanoparticles, such as size and surface, which allow them to interact with or even pass through cell walls or membranes and directly affect intracellular components. The growth and multiplication of many bacteria, including *Bacillus cereus*, *Staphylococcus aureus*, *Citrobacter koseri*, *Salmonella typhi*, *Pseudomonas aeruginosa*, *Escherichia coli*, *Klebsiella pneumonia*, *Vibrio parahaemolyticus*, and *Candida albicans*, are shown to be stopped by Ag nanoparticles by binding Ag/Ag⁺ with the biomolecules [13]. Silver nanoparticles may produce free radicals and reactive oxygen species, which can cause apoptosis and cell death by blocking cell replication.

In the paper [14], investigations were made into the antibacterial properties of the Ag-coated Ti powder. A potential antibacterial effect has been noted. It was also demonstrated that *E. coli* bacteria cannot survive in close proximity to these Ti–Ag surfaces, and the observed antibacterial capabilities may not be connected to the alloy's release of a water-soluble component. Therefore, Ti–Ag alloys are a promising material for antibacterial implants due to their local antibacterial properties, which may also make them biocompatible.

Inorganic AgNO₃-containing sorbents are widely used for the localization of radioactive iodine volatile compounds [15].

The silver-containing sorbents, based on mineral carriers like alumina and silica systems with a meso- and macro-porous structure, are chemically composed to be both hydrophilic and hydrophobic. When compared to analogues, these sorbents are quite inexpensive. Such sorbents can be used in gaseous and liquid media, for example, for thiophenic compounds and mercury adsorption [16, 17]. It should be taken on board that the use of sorbents, catalysts, or composite materials with developed surface area and porosity is a necessary condition for the effective course of a range of heterogeneous processes [18–20].

Therefore, the aim of this study was to obtain promising nanoscale silver-containing antibacterial sorbents using a complex modification of natural Ukrainian zeolites.

2 Experimental

2.1 Synthesis of the Samples

The raw starting material was clinoptilolite zeolite rock from the Sokyrnytsja village deposit in the Transcarpathian region (Ukraine). Clinoptilolite was initially crushed and fractionated. Medium-sized grains (0.5–1.0 mm) were used for further processing. The modification process involved dispersing the zeolite sample in water, adding crystals of ethylenediamine tetraacetic acid (EDTA), and boiling the resulting mixture for three hours. The sample was then washed, its chemical composition was determined, and it underwent further processing four times. The total treatment time was 12 h.

One weight percent of silver was added to the sample by impregnating it with silver nitrate according to its moisture content. Then, the sample was calcined at 480–500 °C for 2 h. A gamma-Al₂O₃ sample with silver was prepared for comparison according to the same modification procedure. Initial gamma-alumina (DSTU 8136-85) was produced by JS “Katalizator” (Kamjanske, Ukraine).

Total viable count (TVC) determination was used to investigate the antibacterial properties of the samples. The TVC was studied using the method of deep sowing of water in nutrient agar according to the methodological instructions “Sanitary and Microbiological Control of Drinking Water” approved by Order of the Ministry of Health of Ukraine No. 60 of the 02/03/2005. All colonies, including microorganisms that grew at 36 °C for 24 h and could be seen at a 2–5 times magnification, were considered. According to the procedure described by the authors’ group, sterilization of nutritional agar was carried out in a microwave oven for 2 min (30 s + 30 s + 1 min) at a radiation strength of 750 W [21].

2.2 Methods

SEM and TEM. Scanning electron microscopy (Zeiss EVO MA 10, Carl Zeiss Microscopy GmbH, Germany) and transmission electron microscopy (JEM 2100F, JEOL, Japan) were used for investigation of samples.

N₂ adsorption. Low temperature nitrogen adsorption/desorption isotherms for samples were measured on a Quantachrome Autosorb NOVA 1200e[®] automatic analyzer (USA) after thermal dehydration in the muffle furnace at 380 °C for 2 h and additional in situ evacuation at 250 °C for 1 h. Utilizing the NOVWin software, the parameters of the porous structure were computed.

X-ray fluorescence (XRF) analysis. The determination of the silver content in the obtained samples as well as the silica-to-alumina ratio was realized using XRF analysis (Oxford Instruments X-Supreme 8000 analyzer, Great Britain).

FTIR spectroscopy. A Shimadzu IR Affinity-1S FTIR spectrometer (Japan) was used to record the FTIR spectra of zeolites in the 400–1500 cm^{-1} region of the framework vibration. The spectral resolution was 2 cm^{-1} .

DTA/TG. Using a Linseis STA 1400 system type derivatograph (Germany), the zeolite samples were subjected to simultaneous thermogravimetric (TG) and differential thermal analysis (DTA) in the temperature range of 20–1000 $^{\circ}\text{C}$. As a reference material, 1200 $^{\circ}\text{C}$ -calcined alumina was used. Every determination was made in a typical atmospheric setting. Each experiment used a sample amount of about 25 mg.

3 Results and Discussion

3.1 Samples Characterization

The first stage of zeolite sample modification involved the EDTA-induced four-fold dealumination/decationation of its pores. Both processes occur simultaneously. After this gentle process, the $\text{SiO}_2/\text{Al}_2\text{O}_3$ ratio changed from 7.3 to 8.7 according to XRF data, the specific surface area (S_{BET}) increased from 11 to 92 m^2/g , and the micropore volume ($V_{\text{t}_{\text{micro}}}$) raised from 0.002 to 0.036 cm^3/g (Fig. 1; Table 1). Furthermore, the latter happened mostly as a result of better access to the sample microporous structure. S_{BET} , micropore surface ($S_{\text{t}_{\text{micro}}}$), and volume ($V_{\text{t}_{\text{micro}}}$) all marginally decreased after Ag impregnation, while overall pore volume (V_{sum}) remained constant. Adsorption properties of the clinoptilolite samples are quite different to those for mordenite–clinoptilolite rocks of Transcarpathia [22, 23] and similar to mineral acid-treated sample of clinoptilolite [24, 25]. In general, natural zeolites are characterized by significantly lower surface areas compared to synthetic zeolites, for which the surface areas according to BET are up to several hundred square meters per 1 g [26, 27].

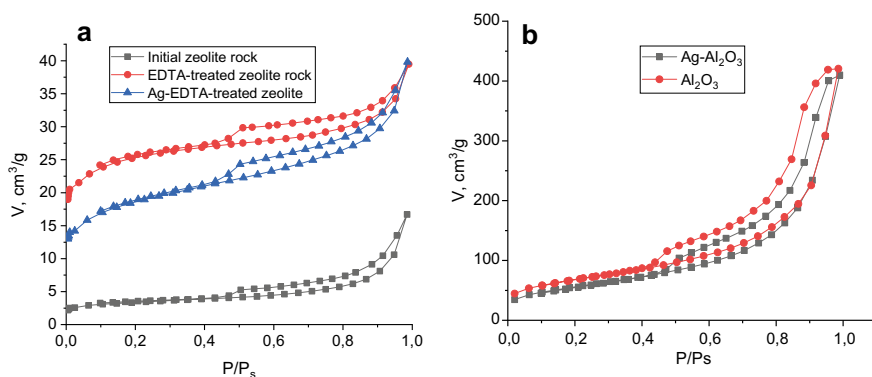


Fig. 1 Low temperature nitrogen adsorption/desorption isotherms for synthesized zeolite (a) and alumina (b) samples

Table 1 Adsorption properties of the samples

Sample	S_{BET} , m ² /g	$S_{\text{t, micro}}$, m ² /g	$V_{\text{t, micro}}$, cm ³ /g	V_{sum} , cm ³ /g
Initial zeolite	11	5.5	0.002	0.031
EDTA-treated zeolite	92	79	0.037	0.0621
Ag-EDTA-zeolite	69	55	0.026	0.061
Al ₂ O ₃	221	7	0.01	0.651
Ag-Al ₂ O ₃	201	6	0.002	0.634

SEM images of the initial zeolite rock and dealuminated zeolite samples (Fig. 2a, b) show typical crystals for natural zeolites [28–31], but images of the initial sample show some impurities on the zeolite crystals, which were removed after EDTA treatment. Some external surface additions we can see after Ag impregnation on zeolite (Fig. 2d, e). It is interesting that in the case of the zeolite sample, we have some cloud-like Ag species and some nanoparticles, whose dimensions are difficult to determine from SEM images. On the alumina sample, only cloud-like species are formed in spite of the same procedure for their preparation (Fig. 2f).

Figure 3 displays TEM images of initial clinoptilolite rock (a), EDTA-treated sample with Ag nanospecies (b, c), and an alumina sample after silver impregnation of Ag-Al₂O₃ (d). Clinoptilolite is the main phase in the initial rock, but it also contains mordenite and magnetite as impurities. Despite XRF analysis confirming the presence of 1 wt% of silver on the alumina sample, silver nanoparticles are not visible in TEM images (d). On clinoptilolite, however, we can see many nanoparticles measuring 5–10 nm. It is known that silver nitrate decomposition is negligible below the melting point, but becomes appreciable around 250 °C and fully decomposes at 440 °C with Ag(0) formation. Silver oxide cannot be formed because it decomposes at a lower temperature than silver nitrate, so the decomposition of silver nitrate yields elemental silver instead. Why we do not see Ag species in the case of Ag-Al₂O₃? With the purpose of understanding these peculiarities, an Ag-Al₂O₃ sample was additionally washed, and the water after treatment was analyzed for Ag-ion presence. The reaction was negative. Therefore, silver nitrate is absent on the sample. Silver nitrate, on the other hand, can react with amphoteric alumina to form AgOH. The latter hydrolyzes to Ag₂O oxide after being washed with hot water. The Ag-Al₂O₃ sample became gray after that. Thus, under the same conditions of impregnation and thermal decomposition of silver nitrate on aluminum oxide, the formation of visible silver nanoparticles is not observed. Obviously, silver forms a powdery or porous layer on the alumina, which can be seen on SEM images as clouds.

Figure 4 shows the FTIR spectra of initial and EDTA-treated zeolite rock in the region of lattice vibrations. The spectrum of the sample did not undergo significant changes after processing, which indicates the absence of sample amorphization and the preservation of its crystalline structure. However, there is a shift of absorption bands of antisymmetrical valence vibrations of the (Si,Al)-O bond at 1015 cm⁻¹ for the initial sample into the high-frequency region to 1035 cm⁻¹, which is associated with an increase in the proportion of silicon, that is, the silica-to-alumina ratio. This

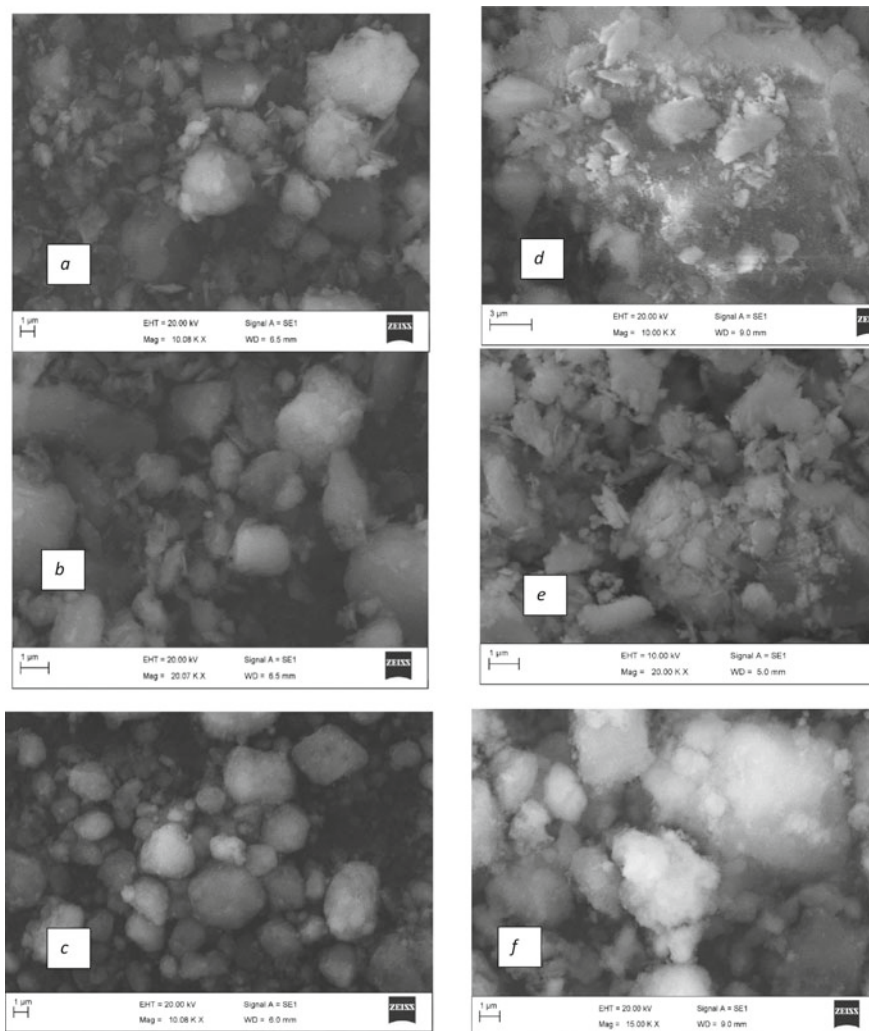


Fig. 2 SEM images of synthesized samples: **a** initial zeolite; **b** EDTA-treated zeolite; **c** Al_2O_3 ; **d**, **e** Ag-EDTA-zeolite; **f** Ag- Al_2O_3

is consistent with the postulate of Woiciehowska et al. [32]: The higher the Si/Al ratio, the band-specific ring oscillations shift toward higher frequencies.

The original form of the clinoptilolite rock and the EDTA-teared sample were investigated using the DTA/TG method. Figure 5 shows the corresponding curves. It is known that the loss of water from zeolite samples often takes place between 100 and 400 °C, and it may be seen in the DTA profiles as an extended endothermic effect [29, 33].

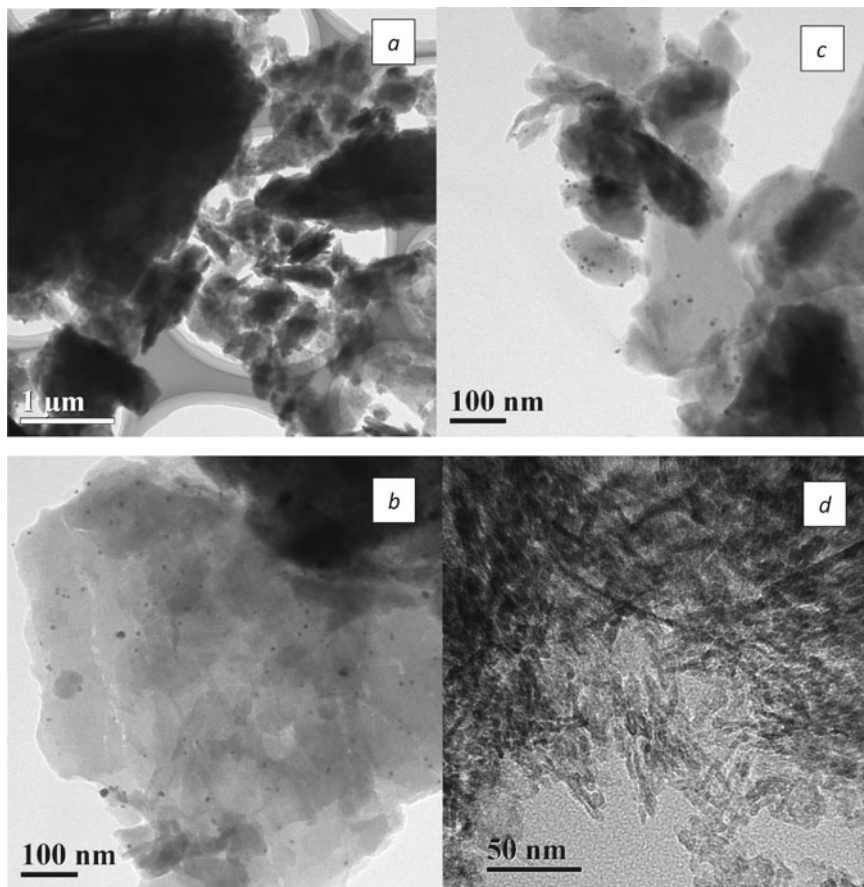
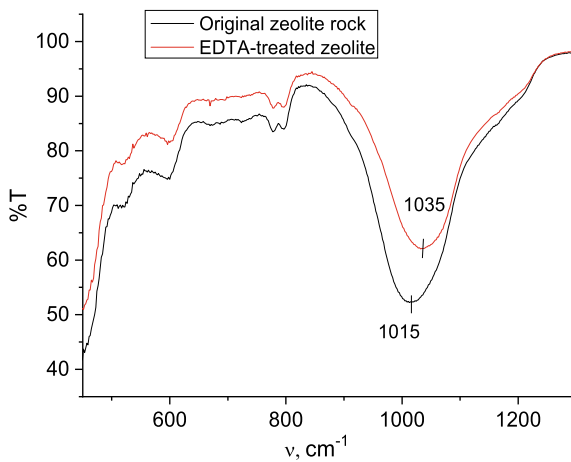


Fig. 3 TEM images: **a** initial zeolite; **b, c** Ag-EDTA-zeolite; **d** Ag-Al₂O₃

Fig. 4 FTIR spectra of initial and EDTA-treated zeolite



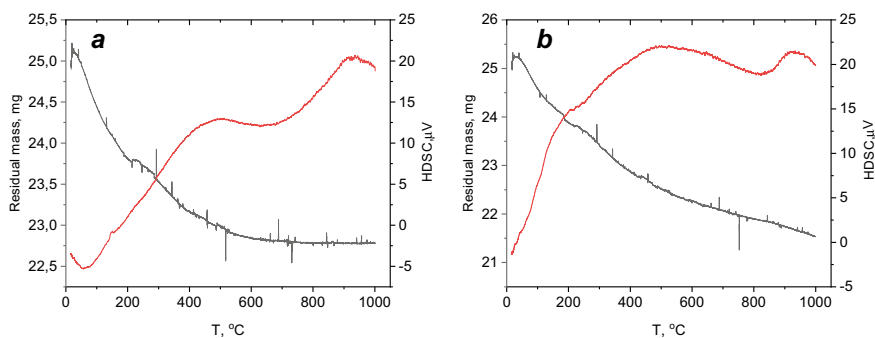


Fig. 5 DTA and TG results for original clinoptilolite zeolite rock (a) and EDTA-treated zeolite (b)

The original rock is characterized by an endotherm near 100 $^{\circ}\text{C}$ related to the dehydration process. The dehydration rate is substantially higher in the original sample than in the treated sample. For the first sample, dehydration is stopped at 500 $^{\circ}\text{C}$, whereas for EDTA-treated zeolite, the dehydration process smoothly follows by the dehydroxylation of acid sites, which is triggered after acid treatment. In the case of original rock, there are no acid sites, and only dehydration takes place. Clinoptilolite zeolite is one of the most thermally stable natural minerals that does not show major structural changes until 800–900 $^{\circ}\text{C}$, but a phase transition process, indicated by an exothermic effect on the DTA curve, is observed at temperature close to 900 $^{\circ}\text{C}$.

3.2 Antibacterial Properties

To determine the starting point of bacterial contamination, the water of three of Kyiv's lakes (Sonyachne, Svyatoshynske, and Radunka) was previously examined. Water samples were tested in June 2022. The initial characteristics of the water samples were as follows: Lake Radunka—70–200 colony-forming units per cm^3 (CFUs/ cm^3); Lake Svyatoshynske—150–250 CFUs/ cm^3 ; Lake Sonyachne—1350–3100 CFUs/ cm^3 . According to TVC values, Lake Radunka water meets standards for both drinking water (up to 100 CFUs/ cm^3 of water) and open water bodies (up to 1000 CFUs/ cm^3 of water). The warnings for Lake Svyatoshynske water are a little more ominous. Thus, Lake Sonyachne water ended up being the worst. Therefore, this water sample was selected for further study.

In Table 2, we have the results of deep sowing of water into peptone-yeast agar in the presence of 0.1 or 0.2 g of zeolite and alumina samples with silver. Using Ag-zeolite increases the purification of water samples by 60–200 times. As a result, according to this indicator, the water sample now fully meets the regulations for

Table 2 Results of the deep sowing of water into nutrient agar in the presence of zeolite and alumina oxide samples

Sample	The number of microorganisms, CFUs/cm ³	
	0.1 g	0.2 g
Ag-EDTA-zeolite	51	16
Ag-Al ₂ O ₃	225	90
Initial water	3010	

surface water and, moreover, even the regulations for drinking water. Then, Ag-alumina requires only 13 and 30 times as much water for purification. Such peculiarities can be caused by different states of applied silver particles, which are both nanoscale and cloud-like in the case of zeolite and only cloud-like in the case of alumina. But we cannot deny the role of Ag species' interactions with zeolite matrix, too. It is known, that the Si–O–Si groups are one of the clinoptilolite functional groups with which heavy metals interact [34]. This interaction can be like the interaction of Brönsted and Lewis acid sites in zeolites and Brönsted/Lewis acid sites with metal species that promote high zeolite acidity and activity [19, 36]. Ag nanoparticles that localize near zeolites exchange cations can be stabilized by cations, which additionally improve their antibacterial properties.

The effect of different sizes of silver nanoparticles on the zeolite matrix on antimicrobial properties and possible silver aggregation requires further investigation.

These conclusions are consistent with the findings of a group of authors [36–38] who discovered that the Ag-clinoptilolite composite has a strong antimicrobial effect against gram-negative bacteria and yeasts, as well as a significant effect on the vital activity of *S. aureus*. It was determined also that the native form of clinoptilolite has a better antibacterial effect against *E. coli* than its H-form. However, antagonistic activity against *S. aureus* was worse than against *E. coli* in both forms. When different forms of clinoptilolite are combined with Ag(I), their antibacterial activity is increased [37, 38].

4 Conclusions

The chemical modification of the Transcarpathian clinoptilolite rock with EDTA resulted in the soft dealumination of the rock, the removal of impurities, and a significant improvement of its porous properties according to the results of low temperature nitrogen adsorption. Ag nanoparticles of 5–10 nm on the zeolite surface can be obtained by impregnation with silver nitrate, followed by the thermal decomposition of the latter, in contrast to a gamma-alumina sample. A considerable drop in the values of total viable count of lake water suggests the potential of Ag-zeolite application in the purification of not only surface water, but drinking water too. In comparison with Ag–Al₂O₃, which also demonstrates some antibacterial properties,

Ag-containing zeolite samples demonstrate better performance in antibacterial properties. The latter can be caused by the nanodimensionality of Ag species as well as the stronger interaction of silver with zeolite cations.

Acknowledgements The authors acknowledge the assistance and support of I. M. Frantsevych Institute for Problems of Materials Science of National Academy of Sciences in conducting the electron transmission microscopy experiments.

References

1. K. Stocker, M. Ellersdorfer, M. Lehner, J.G. Raith, Characterization and utilization of natural zeolites in technical applications. *Berg Huettenmaenn. Monatsh.* **162**, 142–147 (2017). <https://doi.org/10.1007/s00501-017-0596-5>
2. M. Krol, Natural versus synthetic zeolites. *Crystals* **10**, 622–630 (2020). <https://doi.org/10.3390/cryst100706223>
3. Z.O. Znak, S.A. Kornii, A.S. Mashtaler, O.I. Zin, Production of nanoporous zeolites modified by silver ions with antibacterial properties. *Mater. Sci.* **56**, 536–543 (2021). <https://doi.org/10.1007/s11003-021-00461-1>
4. Z.Y. Ji, J.S. Yuan, X.G. Li, Removal of ammonium from wastewater using calcium form clinoptilolite. *J. Hazardous Mater.* **141**, 483–488 (2007). <https://doi.org/10.1016/j.jhazmat.2006.07.010>
5. T. Bruna, F. Maldonado-Bravo, P. Jara, N. Caro, Silver nanoparticles and their antibacterial applications. *Int. J. Mol. Sci.* **22**, 7202 (2021). <https://doi.org/10.3390/ijms22137202>
6. L.P. Silva, A.P. Silveira, C.C. Bonatto, I.G. Reis, P.V. Milreu, Silver nanoparticles as antimicrobial agents: past, present, and future, in *Nanostructures for Antimicrobial Therapy: Nanostructures in Therapeutic Medicine Series* (Elsevier, Amsterdam, 2017), pp. 577–596. ISBN 9780323461511
7. J.W. Tong, Case reports on the use of antimicrobial (silver impregnated) soft silicone foam dressing on infected diabetic foot ulcers. *Int. Wound J.* **6**, 275–284 (2009)
8. C.N. Miller, N. Newall, S.E. Kapp, G. Lewin, L. Karimi, K. Carville, T. Gliddon, N.M. Santamaria, A randomized-controlled trial comparing cadexomer iodine and nanocrystalline silver on the healing of leg ulcers. *Wound Repair Regen.* **18**, 359–367 (2010)
9. J.J. Castellano, S.M. Shafii, F. Ko, G. Donate, T.E. Wright, R.J. Mannari, W.G. Payne, D.J. Smith, M.C. Robson, Comparative evaluation of silver-containing antimicrobial dressings and drugs. *Int. Wound J.* **4**, 114–122 (2007)
10. Y.T. Kim, K. Kim, J.H. Han, R.M. Kimmel, Antimicrobial active packaging for food. *Smart Packag. Technol. Fast Mov. Consum. Goods* **76**, 99–110 (2008)
11. Y. Kampmann, E. De Clerck, S. Kohn, D.K. Patchala, R. Langerock, J. Kreyenschmidt, Study on the antimicrobial effect of silver-containing inner liners in refrigerators. *J. Appl. Microbiol.* **104**, 1808–1814 (2008)
12. A. Kedziora, M. Speruda, E. Krzyzewska, J. Rybka, A. Łukowiak, G. Bugla-Płoskonska, Similarities and differences between silver ions and silver in nanoforms as antibacterial agents. *Int. J. Mol. Sci.* **19**, 444 (2018)
13. K.S. Siddiqi, A. Husen, R.A.K. Rao, A review on biosynthesis of silver nanoparticles and their biocidal properties. *J. Nanobiotechnol.* **16**, 14 (2018). <https://doi.org/10.1186/s12951-018-0334-5>
14. L. Somlyai-Sipos, P. Baumli, A. Sycheva, G. Kaptay, E. Szőri-Dorogházi, F. Kristály, T. Mikó, D. Janovszky, Development of Ag nanoparticles on the surface of Ti powders by chemical reduction method and investigation of their antibacterial properties. *Appl. Surf. Sci.* **533**, 147494 (2020). <https://doi.org/10.1016/j.apsusc.2020.147494>

15. B.J. Riley, S. Chong, R.W. Asmussen, A. Bourchy, M.H. Engelhard, Polyacrylonitrile composites of Ag–Al–Si–O aerogels and xerogels as iodine and iodide sorbents. *ACS Appl. Polym. Mater.* **3**(7), 3344–3353 (2021). <https://doi.org/10.1021/acsapm.1c00237>
16. M. Wdowin, M.M. Wiatros-Motyka, R. Panek, L.A. Stevens, W. Franus, C.E. Snape, Experimental study of mercury removal from exhaust gases. *Fuel* **128**, 451–457 (2014). <https://doi.org/10.1016/j.fuel.2014.03.041>
17. Y. Liu, J. Liao, L. Chang, W. Bao, Ag modification of SBA-15 and MCM-41 mesoporous materials as sorbents of thiophene. *Fuel* **311**, 122537 (2022). <https://doi.org/10.1016/j.fuel.2021.122537>
18. F. Rouquerol, J. Rouquerol, K. Sing, *Adsorption by Powders and Porous Solids: Principles, Methodology and Applications* (Academic Press, San Diego, 1999)
19. J. Weitkamp, M. Hunger, in *Introduction to Zeolite Molecular Sieves*, ed. by J. Cejka, H. van Bekkum, A. Corma, F. Schueth (Elsevier, New York, 2007), pp.787–836
20. I. Ivanenko, A. Voronova, I. Astrelin, Y. Romanenko, Structural and catalytic properties of Ni–Co spinel and its composites. *Bull. Mater. Sci.* **42**, 172 (2019). <https://doi.org/10.1007/s12034-019-1854-9>
21. S.M. Hontarenko, A.M. Herasymenko, Method of agar sterilization for biotechnological investigations. *Bioenergetycy* **1**, 36–38 (2019) (in Ukrainian). <https://doi.org/10.47414/be.1.2019.229288>
22. F.M. Bobonich, V.N. Solomakha, V.V. Bobik, Features of the distribution of aluminum in mordeniteclinoptilolite catalysts for the hydroisomerization of n-hexane. *Theoret. Exp. Chem.* **38**(5), 330–334 (2002)
23. L.K. Patrylak, O.P. Pertko, A.V. Yakovenko, Yu.G. Voloshyna, V.A. Povazhnyi, M.M. Kurmach, Isomerization of linear hexane over acid-modified nanosized nickel-containing natural Ukrainian zeolites. *Appl. Nanosci.* **12**, 411–425 (2022). <https://doi.org/10.1007/s13204-021-01682-1>
24. O. Korkuna, R. Leboda, J. Skubiszewska-Zieba, T. Vrublevska, V.M. Gunko, J. Ryczkowski, Structural and physicochemical properties of natural zeolites: clinoptilolite and mordenite. *Micropor. Mesopor. Mater.* **87**, 243–254 (2006). <https://doi.org/10.1016/j.micromeso.2005.08.002>
25. L. Patrylak, S. Konovalov, A. Yakovenko, O. Pertko, V. Povazhnyi, M. Kurmach, Y. Voloshyna, M. Filonenko, S. Zubenko, Fructose transformation into 5-hydroxymethylfurfural over natural transcarpathian zeolites. *Chem. Chem. Technol.* **16**(4), 521–531 (2022)
26. L.K. Patrylak, M.M. Krylova, O.P. Pertko, Y.G. Voloshyna, Linear hexane isomerization over Ni-containing pentasils. *J. Por. Mater.* **26**(3), 861–868 (2019). <https://doi.org/10.1007/s10934-018-0685-1>
27. L. Patrylak, M. Krylova, O. Pertko, Y. Voloshyna, A. Yakovenko, n-Hexane isomerization over nickel-containing mordenite zeolite. *Chem. Chem. Technol.* **14**(2), 234–238 (2020). <https://doi.org/10.23939/chcht14.02.234>
28. Z. Znak, O. Zin, A. Mashtaler, S. Korniy, Y. Sukhatskiy, R. Gogate Parag, R. Mnykh, P. Thanekar, Improved modification of clinoptilolite with silver using ultrasonic radiation. *Ultrason. Sonochem.* **73**, 105496 (2021). <https://doi.org/10.1016/j.ultsonch.2021.105496>
29. N. Mansouri, N. Rikhtegar, H.A. Panahi, B.K. Shahraki, Porosity, characterization and structural properties of natural zeolite-clinoptilolite-as a sorbent. *Environ. Protect. Eng.* **39**, 139 (2013). <https://doi.org/10.5277/EPE130111>
30. M. Minceva, R. Fajgar, L. Markovska, V. Meshko, Comparative study of Zn²⁺, Cd²⁺, and Pb²⁺ removal from water solution using natural clinoptilolitic zeolite and commercial granulated activated carbon. Equilibrium of adsorption. *Separation Sci. Technol.* **43**, 2117–2143 (2008). <https://doi.org/10.1080/01496390801941174>
31. J.L. Sihombing, S. Gea, A.N. Pulungan, Y.A. Hutapea, The characterization of Sarulla natural zeolite crystal and its morphological structure, in *AIP Conference Proceedings, The 3rd International Seminar on Chemistry: Green Chemistry and its Role for Sustainability* vol. 2049, no. 1 (2018), p. 020062. <https://doi.org/10.1063/1.5082467>

32. K.M. Wojciechowska, M. Król, T. Bajda, W. Mozgawa, Sorption of heavy metal cations on mesoporous ZSM-5 and mordenite zeolites. *Materials* **12**, 3271 (2019). <https://doi.org/10.3390/ma12193271>
33. M. Afzal, G. Yasmeen, M. Saleem, P.K. Butt, A.K. Khattak, J. Afzal, TG and DTA study of the thermal dehydration of metal-exchanged zeolite-4A samples. *J. Therm. Anal. Calorim.* **62**, 721–727 (2000). <https://doi.org/10.1023/A:1026725509732>
34. M.E. Argun, Use of clinoptilolite for the removal of nickel ions from water: kinetics and thermodynamics. *J. Hazard. Mater.* **150**, 587–595 (2008). <https://doi.org/10.1016/j.jhazmat.2007.05.008>
35. L.K. Patrylak, I.A. Manza, V.I. Vypirailenko, A.S. Korovitsyna, R.V. Likhnevskii, Study of the mechanism of hexane isomerization under micropulse conditions. *Theoret. Exp. Chem.* **39**, 263–267 (2003). <https://doi.org/10.1023/A:1025729530977>
36. V.O. Vasylechko, V.O. Fedorenko, O.M. Gromyko, G.V. Gryshchouk, Y.M. Kalychak, O.A. Zaporozhets, M.T. Lototska, Solid phase extractive preconcentration of silver from aqueous samples and antimicrobial properties of the clinoptilolite-Ag composite. *Adsorpt. Sci. Technol.* **35**, 602–611 (2017). <https://doi.org/10.1177/0263617417703509>
37. V.O. Vasylechko, V.O. Fedorenko, O.M. Gromyko, G.V. Gryshchouk, Y.M. Kalychak, S. Tistechol, I. Us, A. Tusyp, A novel solid-phase extraction method for preconcentration of silver and antimicrobial properties of the Na-clinoptilolite-Ag-composite. *Mater Today: Proceed.* **35**, 548–551 (2021). <https://doi.org/10.1016/j.matpr.2019.10.049>
38. V.O. Vasylechko, V.O. Fedorenko, O.M. Gromyko, G.V. Gryshchouk, Y.M. Kalychak, S. Tistechol, I. Us, A. Tusyp, Sorption preconcentration of silver for atomic absorption analysis and antibacterial properties of the acid-modified clinoptilolite-Ag composite. *Methods Objects Chem. Anal.* **15**, 73–82 (2020). <https://doi.org/10.17721/moca.2020.73-82>